Biosensors and Bioelectronics 52 (2014) 427–432

Contents lists available at ScienceDirect

Biosensors and Bioelectronics

journal homepage: www.elsevier.com/locate/bios

A wireless and sensitive detection of octachlorostyrene using modified AuNPs as signal-amplifying tags

Lan Chen [a,b], Jiezhen Li [a], T.Tran ThanhThuy [a,c], Liping Zhou [a], Chen'an Huang [a], Lijuan Yuan [a], Qingyun Cai [a,*]

[a] State Key Laboratory of Chemo/Biosensing and Chemometrics, Department of Chemistry, Hunan University, Changsha 410082, People's Republic of China
[b] Changsha Municipal Drainage Co.,Ltd., Changsha 410003, People's Republic of China
[c] Department of Chemistry, Industrial University of Ho Chi Minh City, Ho Chi Minh, Vietnam

ARTICLE INFO

Article history:
Received 7 May 2013
Received in revised form
15 August 2013
Accepted 16 August 2013
Available online 11 September 2013

Keywords:
Octachlorostyrene
Wireless
Immunosensor
AuNPs
Amplify

ABSTRACT

A wireless, remote query octachlorostyrene (OCS) biosensor was fabricated by coating a mass-sensitive magnetoelastic ribbon with anti-OCS antibody. In response to a time-varying magnetic field, the magnetoelastic sensor mechanically vibrates at a characteristic resonance frequency which inversely depends on the sensor mass loading. As the magnetoelastic film is magnetostrictive itself, the vibrations launch magnetic flux that can be remotely detected using a pickup coil. Au nanoparticles (NPs) were used to amplify the mass loading. In a sample solution containing OCS target and OCS-modified AuNPs (OCS–AuNPs), both OCS and OCS–AuNPs react with the anti-OCS antibody immobilized on the sensor surface in a competition mode. The bound OCS–AuNPs amount is inversely proportional to the OCS target concentration. The reduction of bound OCS–AuNPs induced by free OCS results in significant change in mass loading, which amplifies the responses. The biosensor demonstrates a linear shift in resonance frequency with OCS concentration between 7.4 μM and 9 nM, with a detection limit of 2.8 nM.

1. Introduction

Octachlorostyrene (OCS) is a byproduct of the manufacture of many chlorinated hydrocarbons and belongs to the primary level I group chemicals, which is categorized by the US Environmental Protection Agency (US EPA, 2002) as the most hazardous among the persistent, bioaccumulative, and toxics (PBTs). Even though it has never been commercially used, it is widely distributed in the environments and has been consistently found in fish and sediment samples collected near incineration areas or near potential point sources. Despite the importance of OCS toxicity in aquatic ecosystems, very few articles have studied OCS (Kim and Choung, 2009; Lee and Choi, 2009; Lee et al., 2008; Park and Park, 2008), especially for its detection methods. Most of the detection methods focus on gas chromatography or liquid chromatography coupled with mass spectrometry (Bush et al., 1983; Kuehl et al., 1981; Van Den Brink and De Ruiter-Dijkman, 1997). However, they are unsuitable for field test because of the requirement of expensive instruments and time-consuming sample preparation.

Magnetoelastic sensor is a wireless mass-sensitive platform which has been designed for chemical sensing (Zorn et al., 2003) and biological sensing (Ruan et al., 2003a, 2003b). Critical features of the sensor platform are low cost (approximately $0.001/sensor), making practical use of the sensors on a disposable basis, ease of use, excellent target sensitivity, as well as specificity. The fundamental operating principle of the magnetoelastic sensors involves a change in sensor resonance frequency due to mass loading of the sensor, which herein is associated with binding of an analyte to a receptor immobilized on the surface of the ribbon-like magnetoelastic sensor. In response to a time-varying magnetic field, the magnetoelastic ribbon longitudinally vibrates at a fundamental characteristic resonance frequency f_r that inversely depends on the sensor length L, with width and thickness much smaller than length, Young's modulus E, and density ρ (Landau and Lifschitz, 1986; Stoyanov and Grimes, 2000)

$$f_r = \sqrt{\frac{E}{\rho}}\frac{1}{2L} \tag{1}$$

A small mass load Δm evenly deposited on a sensor of mass M shifts the measured resonant frequency by (Schmidt and Grimes, 2001; Stoyanov and Grimes, 2000):

$$\Delta f = -\frac{f_r}{2}\frac{\Delta m}{M} \tag{2}$$

where M is the mass of the sensor and Δm the mass change.

* Corresponding author. Tel.: +86 731 88821848; fax: +86 731 88821848.
E-mail address: qycai0001@hnu.edu.cn (Q. Cai).

0956-5663/$ - see front matter © 2013 Published by Elsevier B.V.
http://dx.doi.org/10.1016/j.bios.2013.08.026

The frequency shift is downward with increasing mass, $\Delta f = f_{\text{mass-loaded}} - f_r < 0$. The magnetoelastic qualities of the sensor, high permeability and magnetization with low coercive force, enable efficient conversion of the applied magnetic field energy into elastic energy, inducing the sensor to mechanically vibrate. Since the magnetoelastic ribbon is also magnetostrictive, the mechanical vibrations, in turn, generate a magnetic flux density that extends above the sensor and can be detected by a remotely placed pickup coil. Fig. 1 illustrates the operating setup for the wireless magnetoelastic sensing measurements.

The wireless feature, as well as the small sensor size (a few millimeters to a few centimeters) and low material cost make it suitable for applications in various fields, especially where disposable sensors are of the utmost utility. Various magnetoelastic sensors have been reported, including detection of glucose (Cai et al., 2004; Gao et al., 2007), *Escherichia coli* O157:H7 (Huang et al., 2008), *Pseudomonas aeruginosa* (Pang et al., 2007), and polycyclic aromatic hydrocarbons (PAHs) (Lin et al., 2010).

In this work a magnetoelastic OCS biosensor was proposed based on the competitive immunoreaction of the anti-OCS antibody with OCS and OCS–AuNPs. The Au nanoparticles were used to amplify the sensor responses which would lead to more than 1000-fold enhancement in sensitivity (He et al., 2000). To our knowledge, this experiment comprise the first example of adapting modified AuNPs, with wireless magnetoelastic sensor, as a target competitor to amplify the mass change associated with antigen–antibody binding events, in turn significantly increasing the sensitivity of the biosensor.

2. Experiments

2.1. Materials

Magnetoelastic sensors of 18 mM length were cut from a 6 mM wide and 28 nM thick ribbon of Metglas alloy 2826MB ($Fe_{40}Ni_{38}Mo_4B_{18}$) purchased from Honeywell Corporation (Morristown, NJ, USA). The resonance frequency of an uncoated-sensor in air is approximately 120 kHz. Bayhydrol 110, an anionic dispersion of an aliphatic polyester urethane resin in water/N-methyl-2-pyrrolidone solution (50% w/v) was purchased from Bayer Corp. (Pittsburgh, PA). Anti-OCS antibody was derived from immune rabbit preparation in this laboratory. Chloroauric acid ($HAuCl_4$) was obtained from Sigma-Aldrich Chemie Inc. Sodium citrate, sodium borohydride, hydroxylamine hydrochloride, egg albumin (OVA), octachlorostyrene (OCS), tween-20, dichloromethane (CH_2Cl_2) and dimethylsulfoxide (DMSO) were all purchased from commercial sources and used as received. Phosphate buffer solution (PBS) was prepared with NaH_2PO_4 and Na_2HPO_4. Deionized water was used for preparation of all aqueous solutions.

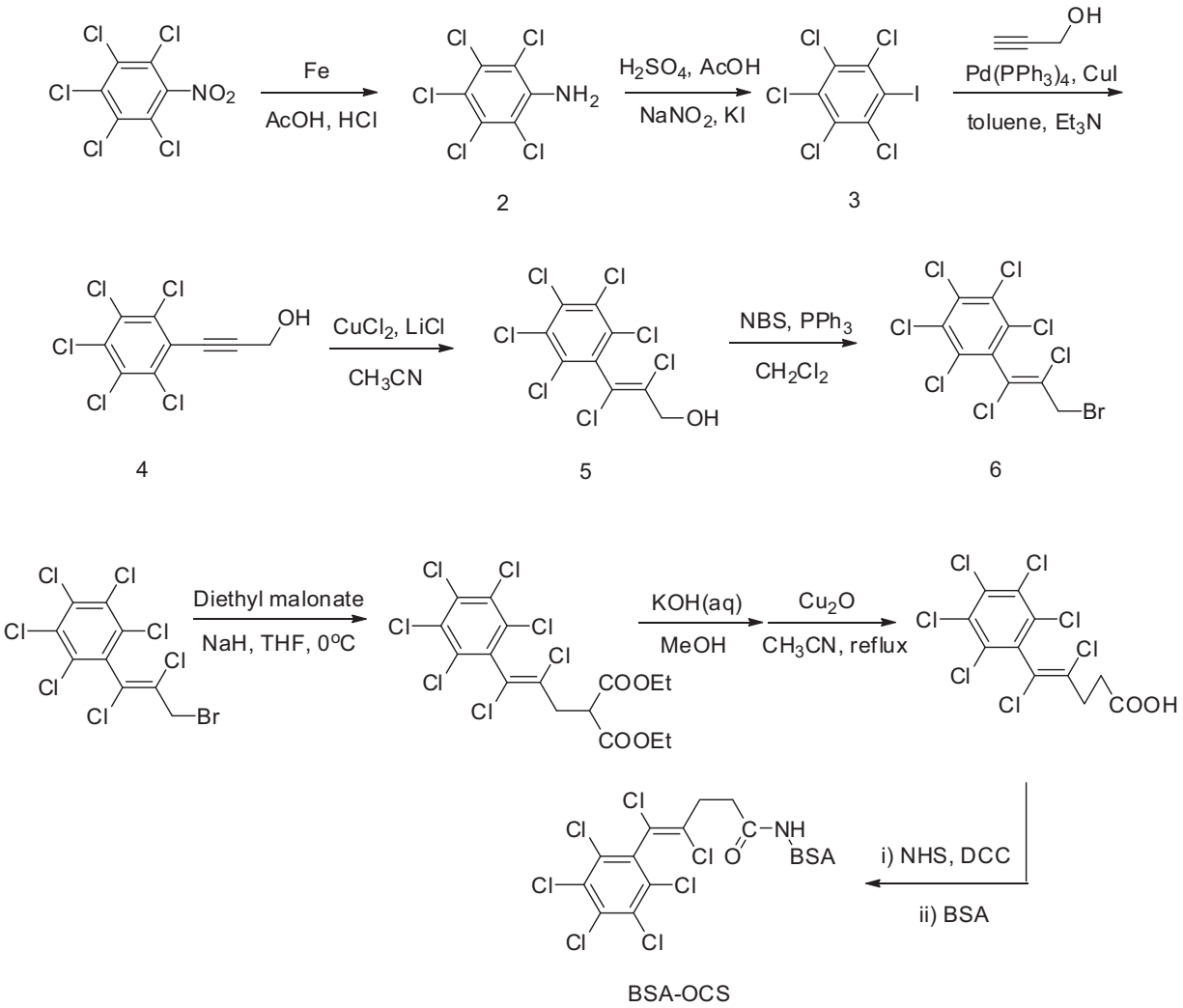

Fig. 1. The synthesis route of immunogen BSA–OCS.

2.2. Apparatus

The spectrum analyzer was from Agilent (Agilent 4395A). All melting points were determined with a Taike XT-4 micromelting-point apparatus. 1H and 13C NMR spectra were recorded on a Varian INOVA-400 instrument using TMS as internal standard. Mass spectra were obtained by SHIMADZU GC-17 QP-5000 or Thermo Finnigan MAT95XP. The morphology and dimension of AuNPs were characterized by scanning electron microscope (SEM; Hitachi S4800) operated at 10 kV. The infrared spectrum was obtained on a FT-IR spectrophotometer (Thermo Nicolet 5700, KBr discs). UV–vis absorption spectrum was obtained with a UV/vis/NIR spectrophotometer (Varian CARY 300 Conc). ^{1}H NMR spectra were recorded on a Varian INOVA-400 instrument using TMS as internal standard. Mass spectra (MS) were obtained by SHIMAZU GC-17 QP-5000 or Thermo Finnigan MAT95XP.

2.3. Sensor fabrication

The magnetoelastic sensor was ultrasonically cleaned in acetone and deionized water each for 20 min. After drying in a stream of nitrogen, about 15 μL of 40% Bayhydrol 110 was applied on both sides of the sensor resulting in a protective film in a thickness of 1 μm. The polyurethane-coated sensors were dried in air and then heated at 150 °C for 2 h to form a robust membrane that protected the iron-rich magnetoelastic substrate from oxidation and corrosion. Then, the polyurethane-protected sensor was immersed in 0.025 M anti-OCS antibody solution at 37 °C for 8 h. After that, it was washed three times by PBS washing buffer (pH 7.4, 0.01 M PBS) containing 0.05% (v/v) tween-20 to remove all unbound anti-OCS antibody, and then blocked with 1% (w/v) OVA/PBS for 4 h. The sensors were stored in refrigerator at 4 °C.

2.4. Immunization and antiserum preparation.

The synthesis route details are reported elsewhere (Shi et al., 2013) and the synthesis route is as simply described in Fig. 1. A male New Zealand white rabbit was immunized for Immunogen BSA–OCS by referring the immunization procedures reported by Shan and Ahn et al. (Ahn et al., 2011; Shan et al., 2000). The final bleed was collected about four months following the first immunization. Blood was collected in test tubes, and blood sample was left to coagulate for 1 h at 37 °C and for 1 h at 4 °C, followed by centrifugation at 10000 rpm for 10 min. Part of the polyclonal antiserum was purified following the previous methods (Kothari et al., 2006). The titer and inhibition of the resulted antibody detected by ELISA were 1:128000 and 32 μg/L, respectively.

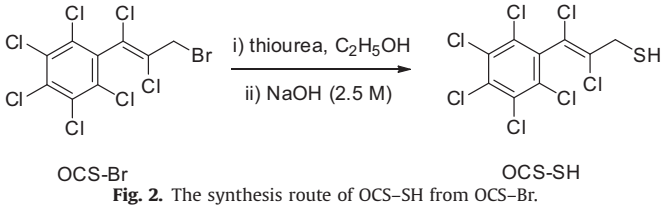

Fig. 2. The synthesis route of OCS–SH from OCS–Br.

2.5. OCS–AuNPs synthesis

OCS–AuNPs were synthesized through a gold-thiolate reaction between OCS–SH and AuNPs. And the OCS-SH was synthesized from OCS-Br as shown in Fig. 2. To a flask containing 20 mL EtOH was added compound OCS–Br (320 mg, 0.73 mmol), followed by thiourea (70 mg, 0.92 mmol) dissolved in 10 mL EtOH. Then the reaction solution was heated to reflux for 12 h. After the solvent was removed in vacuo, the solution of NaOH (88 mg, 2.19 mmol) in 2 mL water was added and heated to reflux for another 2 h. Then the reaction mixture was cooled to room temperature and extracted with ethyl acetate. The extracts were dried (Na_2SO_4), filtered, and concentrated in vacuo. And the residue was purified by a silica gel column as a white solid. The synthesized compounds were characterized by ^{1}H NMR and MS spectra. Product 1: m.p. 55～58 °C; ^{1}H NMR (400 MHz, $CDCl_3$) δ 3.99 (s, 2H), 4.97 (bs, 1H); MS (EI) m/z (%) 387.8 (M^+, 4%), 389.8 (M^++2, 8%), 391.8 (M^++4, 7%), 393.8 (M^++6, 3%), and 395.8 (M^++6, 1%).

AuNPs: Au nanoparticles were synthesized by the reduction of tetrachloroauric acid in trisodium citrate solution with some modifications according to the previously reported method (Haiss et al., 2007). To 90 mL of deionized water, 1 mL of 1 wt% $HAuCl_4 \cdot 3H_2O$ was added, and the mixture was stirred for 1 min; then, 2 mL of 38.8 mM sodium citrate was added, and the reaction mixture was stirred for another minute. A volume of 1 mL of fresh 0.075 wt% $NaBH_4$ in 38.8 mM sodium citrate was added, and the reaction mixture was stirred for 5 min. The as-synthesized AuNPs with a diameter of 10 nM were used as the seed for the preparation of 70 nM Au NPs according to the following process: to 270 mL of water, 6 mL of the Au NPs seed solution was added, followed by the addition of 3 mL 0.2 M $NH_2OH \cdot HCl$. The mixture was stirred vigorously at room temperature, and 2.5 mL of 25.4 mM $HAuCl_4$ was added dropwise to the mixture. The resulting gold colloids were stored at 4 °C in the dark to minimize photoinduced oxidation.

OCS–AuNPs: 200 μL OCS–SH (10^{-5} M in DMSO) was added to 5 mL AuNP solution. The solution was stirred for 12 h at room

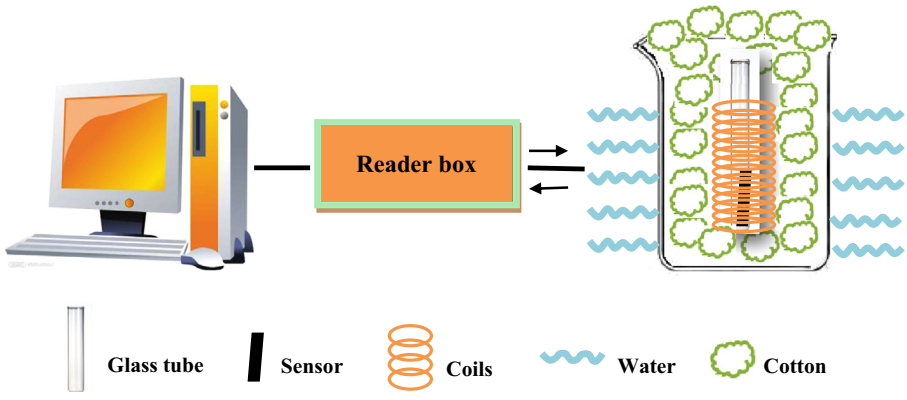

Fig. 3. Schematic showing operation of the wireless magnetoelastic OCS sensor. The sensor is placed within a single coil that serves to both interrogate and detect the sensor. A magnetic field impulse is used to excite the sensor, while the sensor excitation ring-down is analyzed to determine resonance frequency.

temperature. After the surface modification was done, the solution was centrifuged at 5000 rpm for 0.5 h to remove the excess chemicals, and repeated for three times. The OCS–AuNPs was obtained by re-suspending the precipitate in 2 mL of PBS buffer. The concentration of OCS–AuNPs was calculated to be $\sim 10^{-4}$ g/mL by defining the mass of added Au atom versus the ultimate volume as the concentration.

2.6. Measurement

The sensor resonance frequency was detected with the spectrum analyzer. The electronics are capable of resonance frequency determination through frequency counting, damping ratio measurement, and spectrum analysis up to 500 MHz. A computer, connected to the electronics through a RS232 port, coordinates system operation, data display, and data storage. The test setup is schematically shown in Fig. 3. A sensor is placed in a 3 mL glass tube which is inserted into a coil covered by cotton, fixed at the middle of a beaker and the beaker was kept at 37 °C by water bath. The coil launch a time-varying magnetic field and picks up the magnetic flux which is launched by the sensor vibration. The magnetoelastic sensor mechanically vibrates at a characteristic resonance frequency in response to the time-varying magnetic field. In the vial was added 0.8 mL PBS solution containing different concentrations of OCS–AuNPs and target OCS. After incubation at 37 °C for 400 min the resonance frequency of the sensor was detected.

Fig. 4 is a schematic diagram of the immunosensor based on competitive immunoreactions. The sensor was incubated in 0.8 mL of PBS containing different concentrations of OCS–AuNPs and target OCS at 37 °C for a certain time. The OCS–AuNPs and OCS in the testing solution would compete to react with the immobilized anti-OCS antibody. Prior to use, the sensor was activated in 0.01 mol/L pH 7.4 PBS buffer solution for 10 min to wet the polymer. The resonance frequency of the sensor was measured in 60 s intervals by a sensor reader with step frequency 20 Hz, and the volatage amplitude here was 1.8 V.

The frequency shifts in the absence of OCS were recorded as Δf_0, and in the presence of OCS were recorded as Δf_x. OCS was quantified based on the OCS-resulted frequency change (δf)

$$\delta f = \Delta f_x - \Delta f_0 > 0 \quad (3)$$

After each immunoassay and detection, the magnetoelastic sensor was discarded and another new one was used for the next detection.

3. Results and discussions

3.1. Characterizations

The immunosensor was fabricated by physically absorbing the anti-OCS antibody on a polyurethane-protected magnetoelastic film. Fig. S1A (Supplementary information) shows the typical kinetic response of the immunosensor incubating in pH 7.4 PBS buffer containing 0.025 mg/mL anti-OCS antibody. The resonance frequency decreases with increasing the incubation time, and reaches a platform after 8 h incubation, giving frequency shifts of $\sim$1000 Hz. While in blank solution, the sensor remained unchanged, indicating no unspecific adsorption. We make note that the decrease in resonance frequency with the mass loading is associated with the antibody absorption.

Magnetoelastic sensor is a mass sensitive transducer. The detection of OCS is based on the mass change resulted from immunoreaction between the antibodies fixed on sensor surface and free OCS. As for small molecule OCS, the immune binding with OCS would result in insignificant mass change. So it is necessary to use AuNPs to amplify the mass change to improve the sensitivity. The prepared AuNPs with sizes of 70–100 nM in diameter are shown in the SEM image of Fig. S1B. The large particle size is beneficial to the signal amplification. To confirm that OCS–SH was bonded to the AuNPs, UV–visible and FT-IR spectrum (KBr discs) were recorded. Fig. S1C shows that the AuNPs exhibit UV–vis absorption peaks at 559 nM and 321 nM (this peak belongs to the excess $HAuCl_4$ (Eustis et al., 2005), while the OCS–AuNPs have a peak at 561 nM. The surface plasmon resonance (SPR) of AuNPs shifts the absorption slightly from 559 to 561 nM, which is consistent with the difference between AuNPs before and after modifications. FT-IR spectroscopy of AuNPs, OCS, and OCS–AuNPs was recorded in Fig. S1D. The FT-IR spectrum displays characteristic bands of OCS–SH at 748 cm^{-1} (C–Cl), 1370 cm^{-1} (aromatic C=C), 1524 cm^{-1} (ClC=CCl), 2800 cm^{-1}, and 2975 cm^{-1}(CH_2), confirming the modification of OCS–SH on AuNPs.

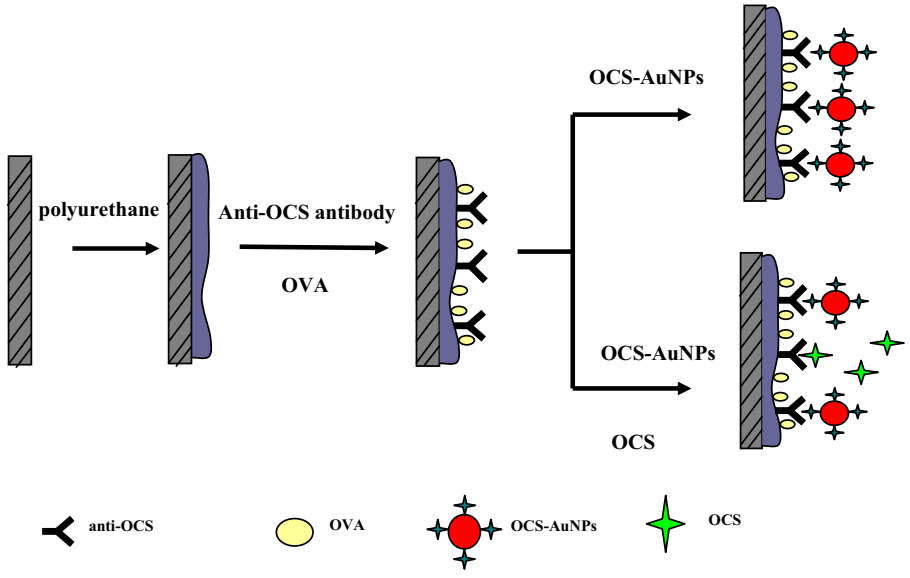

Fig. 4. Schematic representation of the assay procedures of anti-OCS antibodies bonded to magnetoelastic sensor, including incubating OCS and OCS–AuNPs sample, deposition of OCS–AuNPs products onto the sensor surface resulting in a decrease in sensor resonance frequency.

3.2. Optimization of the assay conditions

The assay is greatly influenced by temperature since the binding ability of antibody toward antigen is high related to the temperature. The responses at temperature ranging from 15 to 50 °C were investigated. As shown in Fig. S2A, 37 °C is the optimal temperature at which the largest frequency shift is obtained. Further increase of temperature caused a decrease of the response.

In immune reaction, the target antigen OCS and the OCS–AuNPs compete for the limited number of antibody sites on the sensor surface. The OCS–AuNPs concentration is therefore an important factor to affect the sensitivity. As shown in Fig. S2B, the maximum response is observed while 15 μL OCS–AuNPs are added in 0.8 mL PBS solution containing 1 μM OCS. Basically the optimal OCS–AuNPs concentration is dependent on the OCS concentration. The chosen concentration of OCS (1 μM) is at the upper bound of the linear range. From Fig. S2B one can see that excess OCS–AuNPs cause a less decrease in responses than insufficient OCS–AuNPs. Based on this observation, 15 μL OCS–AuNPs were used in the following assays.

3.3. OCS detection

Fig. 5 shows real-time amplitude–frequency spectra of the magnetoelastic sensor measured in PBS (pH=7.4) containing 5 μM OCS and 15 μL OCS–AuNPs. Both the resonance frequency and amplitude decrease with the incubation time. After 400 min immunoreaction, the binding of OCS–AuNPs on the sensor results in a decrease of 330 Hz in resonance frequency (Δf) and 0.5 V in amplitude. The OCS-resulted change in frequency was used to quantify OCS.

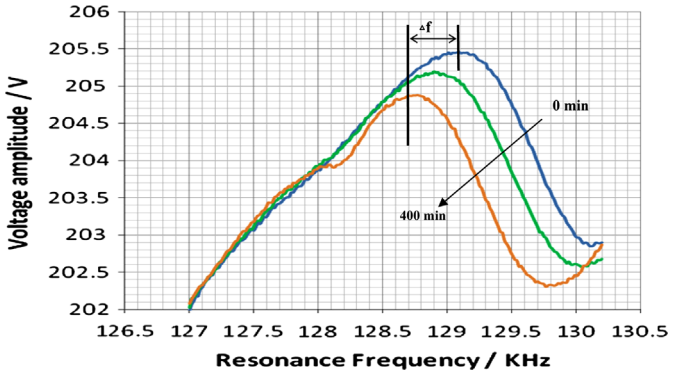

Fig. 5. Real-time frequency spectrum of a sensor in 5 μM OCS solution under optimal experimental conditions.

Because the OCS–AuNPs concentration was fixed, the bonded OCS–AuNPs are inversely proportional to the concentration of OCS in solution. Consequently the resonance frequency of the sensor changes inversely with the concentration of OCS in solution. The time-dependent frequency responses at different OCS concentrations are shown in Fig. 6A. The resonance frequency increases with increasing the OCS concentrations. Fig. 6A curve h shows the response of a blank sensor (without immobilizing the antibody) to OCS–AuNPs, indicating that the nonspecific binding of OCS–AuNPs on the sensor surface can be ignored. A decrease in resonance frequency of approximately 110 Hz is observed over the 400 min test period due to the non-specific adsorption of OCS–AuNPs. The result is similar with previous study concerning the non-specific adsorption of streptavidin on magnetoelastic sensors (Pradier et al., 2002; Ruan et al., 2004).

The standard calibration curve for the determination of OCS on the wireless immune magnetoelastic sensor is shown in Fig. 6B, with the sensitivity calculated from the frequency shift achieved during the first 400 min. A response is linear with the logarithm of OCS concentration in the range from 9 nM to 7.4 μM, which could be represented by the equation $\delta f = 311.2 \log C_{ocs} + 2740$. The limit of detection (LOD) was calculated to be 2.8 nM with taking the three times noise (N) as signal

$$\mathrm{LOD} = 10\,\hat{}\,[(3N - 2740)/311.2] \quad (4)$$

Where the noise is the standard deviation calculated from the blank response curve h in Fig. 6A, the nonspecific absorption curve, which was stable within 400 min period of reaction. Here the N was calculated to be 25 Hz.

3.4. Specificity and reliability

As for a fast-scanning in the site analytical method, the specificity is a key factor to determining its applicability. The sensor responses to compounds with a molecular structure similar to OCS were investigated to evaluate the sensor specificity. The investigated compounds include pentachloroiodobenzene (PCIB), (E)-2,3-dichloro-3-(pentachlorophenyl) prop-2-ene-1-hydroxy (OCS-OH), hexachlorobenzene (HCB), pentachloroaniline (PCA) and pentachloronitrobenzene (PCNB) at concentration of 10^{-7} M. As shown in Fig. S3, all the investigated compounds except OCS-OH show little interference. As OCS-OH is with high similarity with OCS, the sensor response to OCS is only 2.8 times that to OCS-OH.

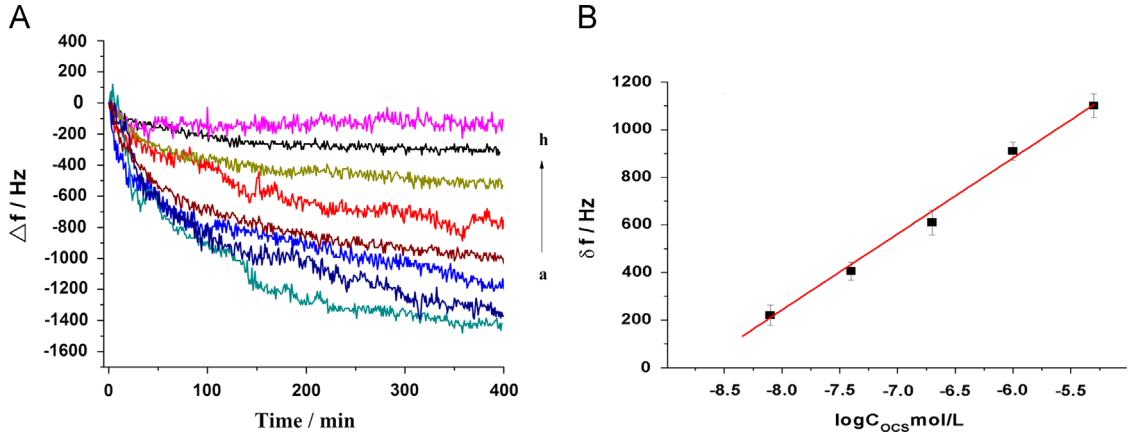

Fig. 6. (A) The time-dependent frequency shift as a function of the initial concentration of OCS: (a–g) 0 M, 1.6×10^{-9} M, 8×10^{-9} M, 4×10^{-8} M, 2×10^{-7} M, 10^{-6} M, and 5×10^{-6} M with 15 μL OCS–AuNPs, and (h) the background noise measured using no-antibody sensor with 15 μL OCS–AuNPs. (B) Calibration curve: δf versus OCS concentrations.

The applicability was further evaluated by recovery rate test. The recovery rates were investigated by analyzing Xiangjiang river water samples spiked with OCS at concentrations of 0.5 nM and 1 nM (Table S1). The water samples were filtered with a filter paper prior to analysis. The spiked water sample was directly applied for the immunoassay. The recovery rate is defined as the ratio of the detected concentration to the added concentration.

The OCS content in Xiangjiang river water was also analyzed. After filtering with a filter paper, 30 mL dichloromethane was added into 500 mL of the collected water samples under stirring for 3 h. Then the organic phase was separated, collected, and dried with a rotary evaporator. The residual was dissolved in 500 μL 5% DMSO for immunoassay. The frequency shift in response to the water sample kept nearly the same as the blank, suggesting that the OCS content in the Xiangjiang river water is under the detection limit of this method. All measurements were replicated for three times. The OCS sensitivity of the magnetoelastic biosensor is comparable with several other biosensor platforms used for detection of small molecules. A few examples are cited here for comparison. A quartz crystal microbalance (QCM) immunosensor for detection of ethyl para-nitro-phenyl and carbofuran is with a LOD of 15.5 nM and 1.3 nM (Kim et al. 2007), respectively. 338 A QCM immunosensor for detection of 3,5,6,-trichloro-2-pyridinol (TCP) is with a LOD of 35 nM (March et al. 2009). A surface LOD of 0.4 nM (Kawazumi et al. 2005). A fluorescence immunosensor for detection of pentachlorophenol (PCP) is with a LOD of 37 nM (Krikounova et al. 2002).

4. Conclusions

A wireless octachlorostyrene (OCS) immunosensor was described based on a mass-sensitive magnetoelastic sensor immobilized with anti-OCS antibody. OCS–AuNPs with heavy molar mass was used to amplify the responses. OCS and OCS–AuNPs competitively bind with the antibodies on the sensor surface. The sensor mass loading is inversely related to the OCS concentration as the result that the loaded heavy OCS–AuNPs decreases with increasing the OCS concentration. A linear response is obtained in the range from 7.4 μM to 9 nM, with a LOD of 2.8 nM for a 400 min incubation period. The sensor shows a high specificity. Since no physical connections between the sensor and the monitoring electronics are required, and the sensor is entirely passive without requiring an internal power supply, this sensor platform offers an exciting opportunity for developing a useful in situ fast scanning technology for OCS measurement.

Acknowledgment

We gratefully acknowledge the National Basic Research Program of China (Grant no. 2009CB421601), the National Science Foundation of China (Grants 21175038 and 21235002) for financial support. We thank the editor and reviewers for helpful comments and suggestions.

Appendix A. Supplementary material

Supplementary data associated with this article can be found in the online version at http://dx.doi.org/10.1016/j.bios.2013.08.026.

References

Ahn, K.C., Kasagami, T., Tsai, H.J., Schebb, N.H., Ogunyoku, T., Gee, S.J., Young, T.M., Hammock, B.D., 2011. Environmental Science and Technology 46 (1), 374–381.
Bush, B., Snow, J., Connor, S., 1983. Association of Official Analytical Chemists Journal 66 (2), 248–255.
Cai, Q., Zeng, K., Ruan, C., Desai, T.A., Grimes, C.A., 2004. Analytical Chemistry 76 (14), 4038–4043.
Eustis, S., Hsu, H.-Y., El-Sayed, M.A., 2005. The Journal of Physical Chemistry B 109 (11), 4811–4815.
Gao, X., Yang, W., Pang, P., Liao, S., Cai, Q., Zeng, K., Grimes, C.A., 2007. Sensors and Actuators B: Chemical 128 (1), 161–167.
Haiss, W., Thanh, N.T., Aveyard, J., Fernig, D.G., 2007. Analytical Chemistry 79 (11), 4215–4221.
He, L., Musick, M.D., Nicewarner, S.R., Salinas, F.G., Benkovic, S.J., Natan, M.J., Keating, C.D., 2000. Journal of American Chemistry Society 122 (38), 9071–9077.
Huang, S., Pang, P., Xiao, X., He, L., Cai, Q., Grimes, C.A., 2008. Sensors and Actuators B: Chemical 131 (2), 489–495.
Kawazumi, H., Gobi, K.V., Ogino, K., Maeda, H., Miura, N., 2005. Sensors and Actuators B: Chemical 108 (1), 791–796.
Kim, N., Park, I.-S., Kim, D.-K., 2007. Biosensors and Bioelectronics 22 (8), 1593–1599.
Kim, S.J., Choung, S.Y., 2009. Archives of Pharmacal Research 32 (11), 1585–1592.
Kothari, H., Kumar, P., Singh, N., 2006. Protein Expression and Purification 45 (1), 15–21.
Krikounova, V.S., Abuknesha, R., Eremin, S.A., 2002. The Scientific World Journal 2, 1132–1137.
Kuehl, D.W., Johnson, K.L., Butterworth, B.C., Leonard, E.N., Veith, G.D., 1981. Journal of Great Lakes Research 7 (3), 330–335.
Landau, L., Lifschitz, E., 1986. Pergamon, New York.
Lee, S.W., Choi, J., 2009. Environmental Toxicology and Pharmacology 28 (2), 269–274.
Lee, S.W., Park, K., Hong, J., Choi, J., 2008. Environmental Toxicology and Chemistry 27 (5), 1118–1127.
Lin, H., Chen, Z., Lu, Q., Cai, Q., Grimes, C.A., 2010. Sensors and Actuators B: Chemical 146 (1), 154–159.
March, C., Manclús, J., Jiménez, Y., Arnau, A., Montoya, A., 2009. Talanta 78 (3), 827–833.
Pang, P., Huang, S., Cai, Q., Yao, S., Zeng, K., Grimes, C.A., 2007. Biosensors and Bioelectronics 23 (2), 295–299.
Park, E.J., Park, K., 2008. Toxicology in Vitro 22 (2), 367–375.
Pradier, C.M., Salmain, M., Zheng, L., Jaouen, G., 2002. Surface Science 502, 193–202.
Ruan, C., Ong, K.G., Mungle, C., Paulose, M., Nickl, N.J., Grimes, C.A., 2003a. Sensors and Actuators B: Chemical 96 (1), 61–69.
Ruan, C., Zeng, K., Varghese, O.K., Grimes, C.A., 2003b. Analytical Chemistry 75 (23), 6494–6498.
Ruan, C., Zeng, K., Varghese, O.K., Grimes, C.A., 2004. Biosensors and Bioelectronics 19 (12), 1695–1701.
Schmidt, S., Grimes, C.A., 2001. Sensors and Actuators A: Physical 94 (3), 189–196.
Shan, G., Leeman, W.R., Stoutamire, D.W., Gee, S.J., Chang, D.P., Hammock, B.D., 2000. Journal of Agricultural and Food Chemistry 48 (9), 4032–4040.
Shi, L., Zhou, L., Dai, G., Wang, N., An, D., Cai, Q., 2013. Talanta.
Stoyanov, P.G., Grimes, C.A., 2000. Sensors and Actuators A: Physical 80 (1), 8–14.
Van Den Brink, N., De Ruiter-Dijkman, E.M., 1997. Antarctic Science 9, 414–417.
Zorn, M.E., Rahne, K.A., Tejedor-Tejedor, M.I., Anderson, M.A., Grimes, C.A., 2003. Analytical Chemistry 75 (22), 6223–6230.